Electronic Supplementary Information

Influence of patch size and chemistry on the catalytic activity of patchy hybrid nonwovens

Christian Hils,[a] *Martin Dulle,*[b] *Gabriel Sitaru,*[c] *Stephan Gekle,*[c] *Judith Schöbel,*[d] *Andreas Frank,*[e] *Markus Drechsler,*[f] *Andreas Greiner,*[a,g] *Holger Schmalz* [a,g,*]

a) University of Bayreuth, Macromolecular Chemistry II, Universitätsstraße 30, 95440 Bayreuth, Germany

b) Forschungszentrum Jülich GmbH, JCNS-1/ICS-1, Wilhelm-Johnen-Straße, 52428 Jülich, Germany

c) University of Bayreuth, Biofluid Simulation and Modeling, Theoretische Physik VI, Universitätsstraße 30, 95440 Bayreuth, Germany

d) University of Groningen, Macromolecular Chemistry & New Polymeric Materials, Zernike Institute for Advanced Materials, Nijenborgh 4, 9747 AG, Groningen, The Netherlands

e) University of Bayreuth, Macromolecular Chemistry I, Universitätsstraße 30, 95440 Bayreuth, Germany

f) University of Bayreuth, Bavarian Polymer Institute, Keylab Optical and Electron Microscopy, Universitätsstraße 30, 95440 Bayreuth, Germany

g) University of Bayreuth, Bavarian Polymer Institute, Keylab Synthesis and Molecular Characterization, Universitätsstraße 30, 95440 Bayreuth, Germany

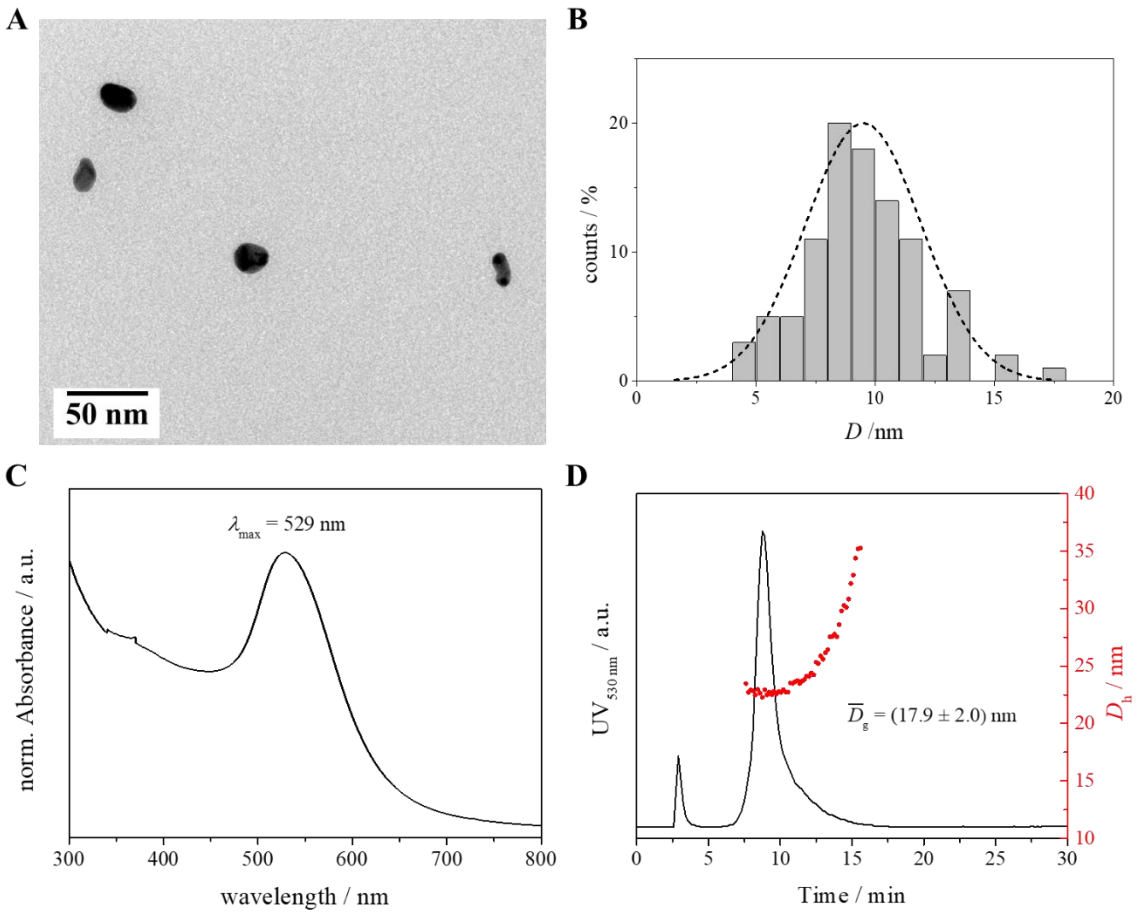

Fig. S1. Characterization of the employed aqueous, citrate-stabilized Au NP dispersion. A) TEM micrograph, B) size distribution with D_{TEM} = 9.5 ± 2.4 nm, C) UV-Vis spectrum and D) AF4 measurement revealing a diameter of gyration of D_g = 17.9 ± 2 nm, using the relation D_g/D_h = 0.775 for solid spheres.

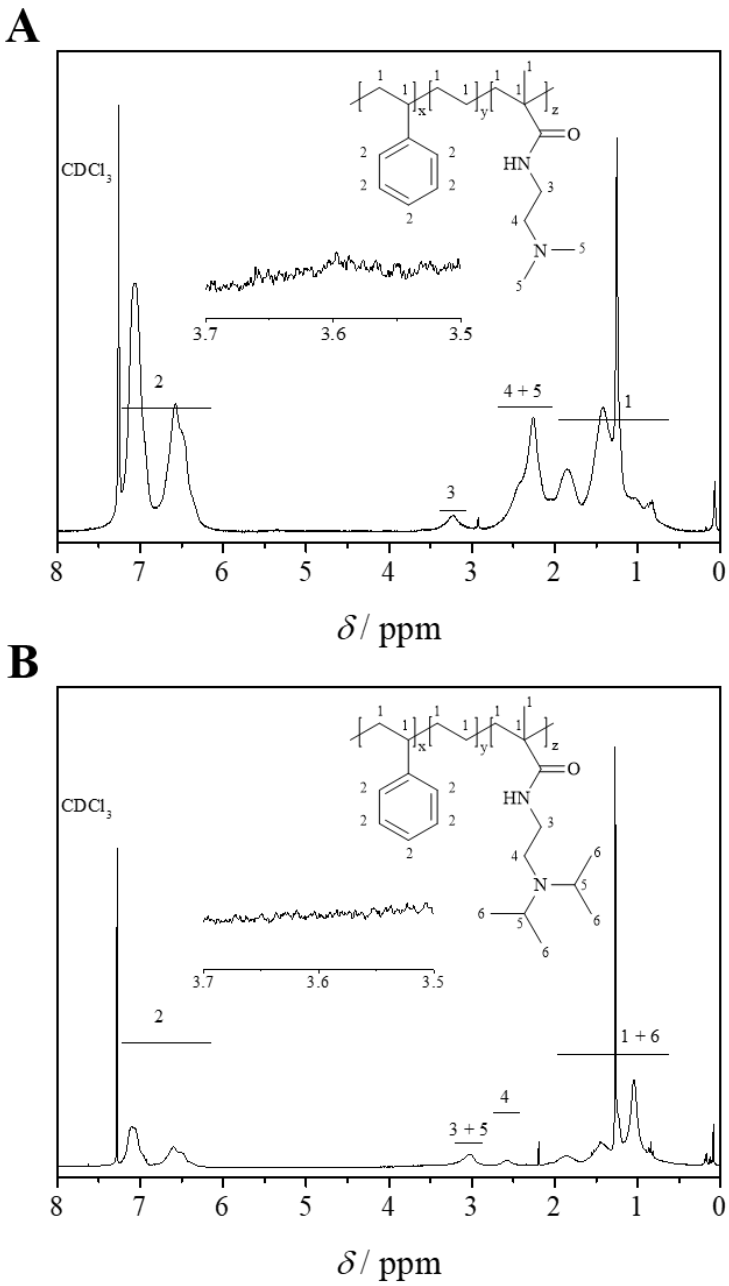

Fig. S2. ^{1}H NMR spectra of A) *s*-SEDMA ($S_{33}E_{17}DMA_{50}^{131}$) and B) *s*-SED*i*PA ($S_{28}E_{15}D\mathit{i}PA_{58}^{156}$) measured in $CDCl_3$. Quantitative conversion in the polymer analogous amidation of the corresponding PS-*b*-PE-*b*-PMMA triblock terpolymer precursor is proven by the absence of methyl ester protons, which would be expected to appear at δ = 3.6 ppm.

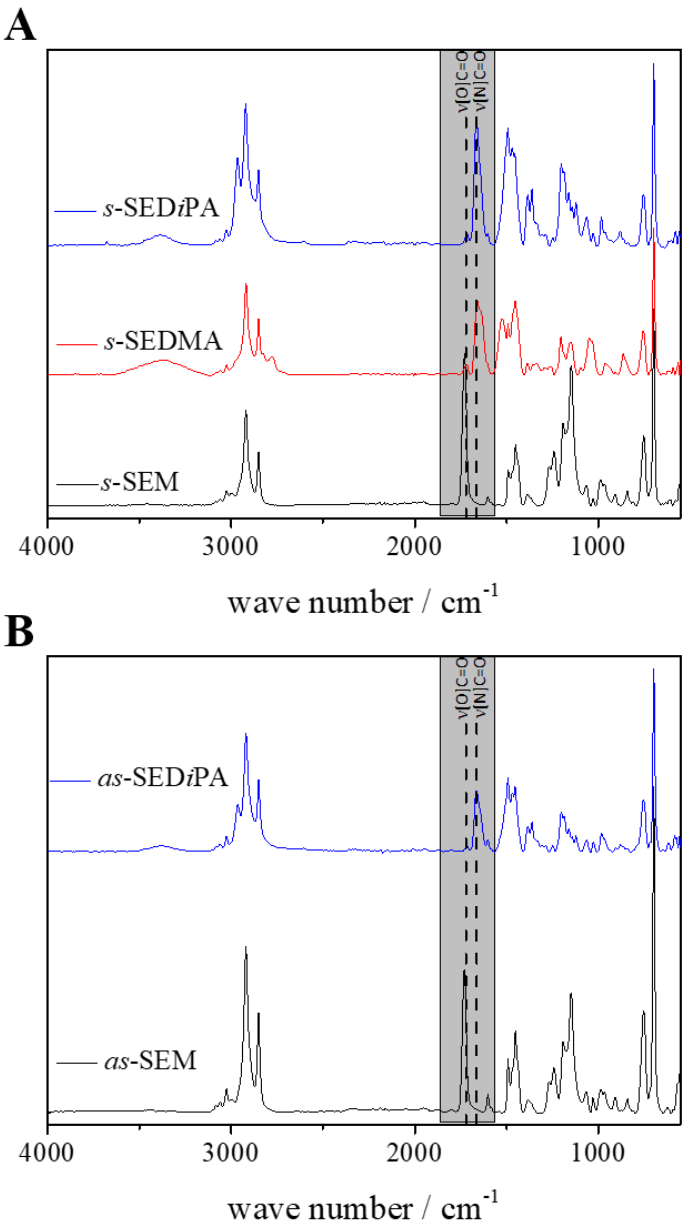

Fig. S3. FT-IR spectra of A) symmetric and B) asymmetric triblock terpolymers. In the FT-IR spectra of the amidated triblock terpolymers the carbonyl stretching vibration (ν[O]C=O) of the methyl ester units of the PS-*b*-PE-*b*-PMMA triblock terpolymer precursor (black spectra) is hardly detectable, confirming a nearly complete conversion.

Table S1. Thermal properties of the amidated triblock terpolymers determined by μDSC.*

triblock terpolymer	T_c [°C]	T_m [°C]
s-SED*i*PA	15	52
as-SED*i*PA	22	47
s-SEDMA	21	53

* c = 10 g·L^{-1} in THF, scanning rate 0.5 K·min^{-1}.

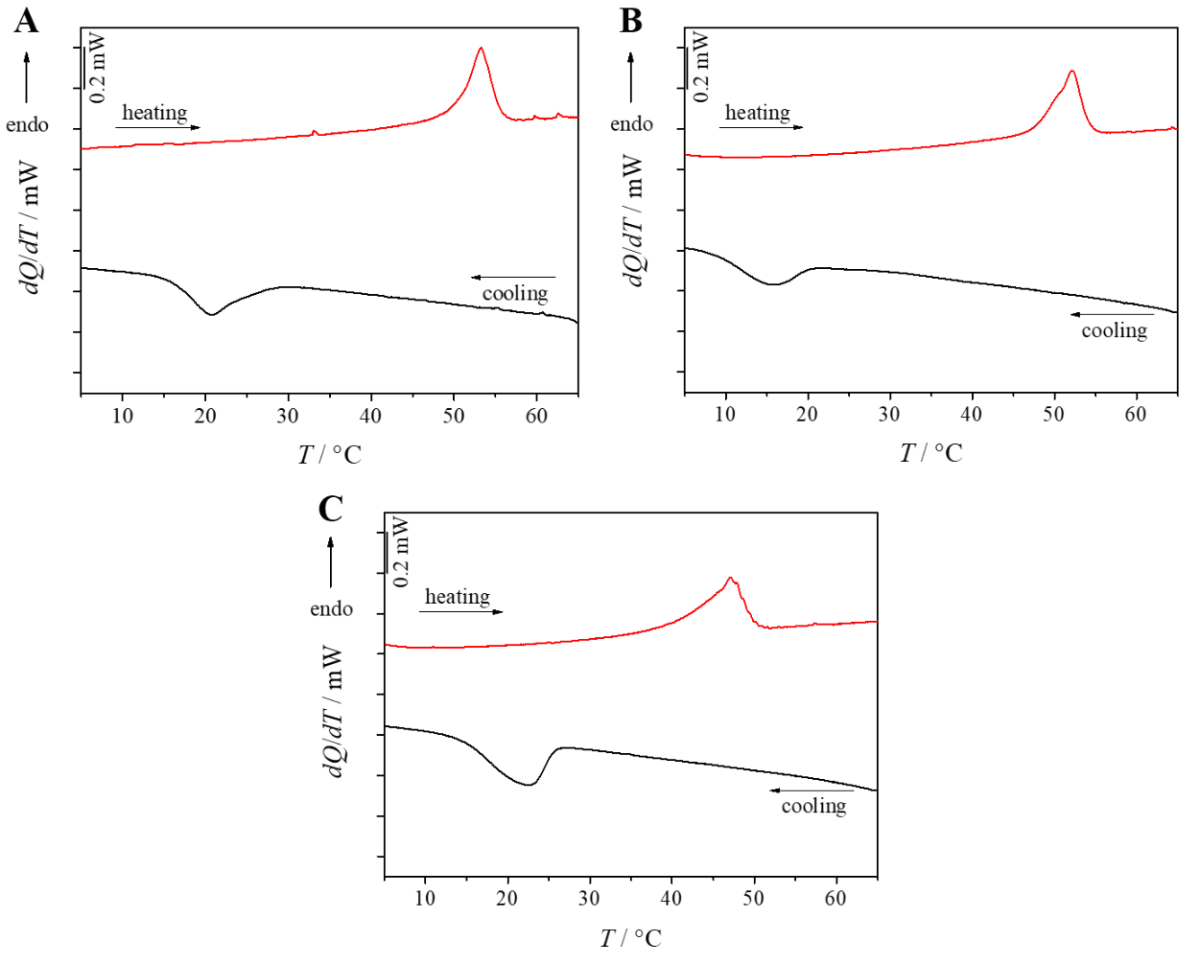

Fig. S4. μDSC heating (red) and cooling (black) traces (c = 10 g·L^{-1} in THF, scanning rate 0.5 K·min^{-1}). A) *s*-SEDMA ($S_{33}E_{17}DMA_{50}^{131}$), B) *s*-SED*i*PA ($S_{28}E_{15}DiPA_{58}^{156}$) and C) *as*-SED*i*PA ($S_{38}E_{21}DiPA_{41}^{181}$).

UV-Vis Measurements. The initial concentration of the Au NP dispersion was determined by ICP-OES measurements ($c_{Au} = 0.50 \cdot 10^{-3}$ mol·L^{-1}). Furthermore, the concentration of elemental gold ([Au]) can be determined directly from the measured UV-Vis spectrum according to eqn (S1), using the absorbance of the Au NP dispersions at a wavelength of λ = 400 nm (A_{400}).[1] The Au content in [µg] ($m_{Au,\ UV\text{-}Vis\ 400nm}$) is then calculated from the respective volume of the dispersion and the molar mass of Au (M_{Au} = 196.97 g·mol^{-1}). In addition, a calibration based on the employed Au NP dispersion was constructed by plotting the absorbance at λ = 400 nm *vs.* the Au content (in [µg]) of the dispersions with different dilutions (Fig. S5). For both methods the amount of embedded gold in the hybrid nonwovens was calculated from the respective Au contents of the dispersions before and after loading (difference method).

$$[Au] = \frac{A_{400} \cdot f \cdot 1.25 \cdot 10^{-4}\ mol \cdot L^{-1}}{0.3} \cdot 100 \qquad \text{(S1)}$$

The dilution factor *f* indicates the dilution of the measured dispersion.[1]

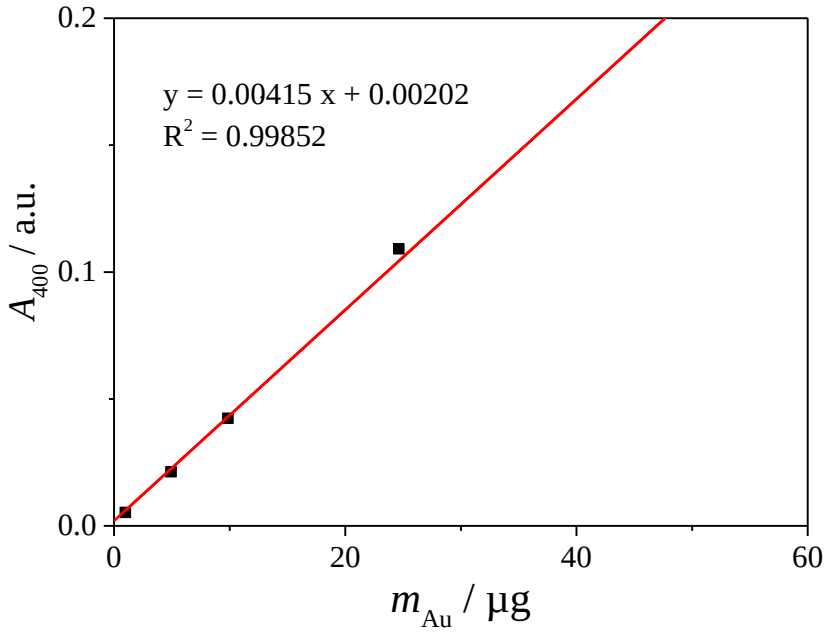

Fig. S5. Calibration line for the determination of the gold content from the absorbance of the employed aqueous Au NP dispersion at λ = 400 nm.

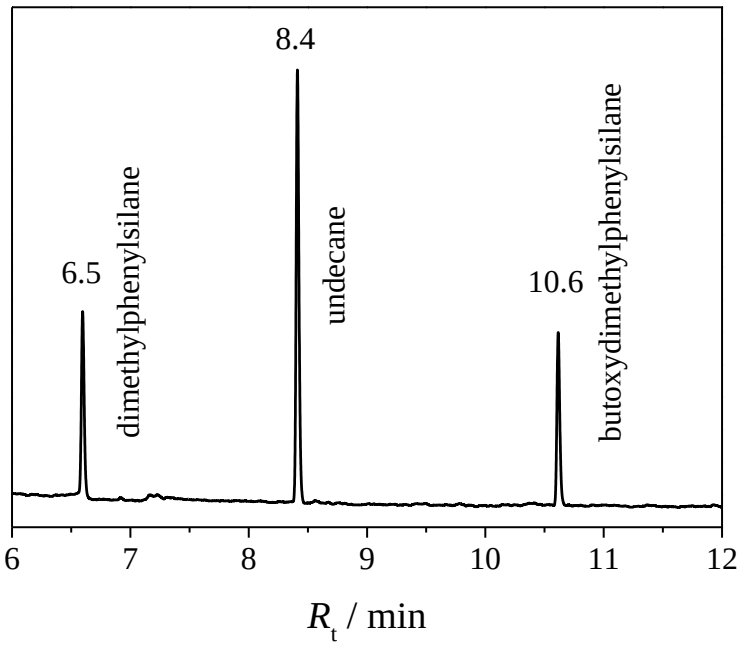

Fig. S6. Representative GC spectrum for the sample taken after 4h in the catalytic alcoholysis of dimethylphenylsilane with NW_s-SEDMA(w)/Au. The assignment of the GC signals was proven by GC-MS (gas chromatography coupled with mass spectrometry) in our previous report.[2]

Determination of patch sizes and average micelle lengths by TEM. The determination of the patch size (red for the amidated and blue for the PS patches) was done with *ImageJ* using the tool "straight line" after setting the scalebar (Fig. S7). The mean average and standard deviation were calculated from 100 patches. The mean length and standard deviation of the worm-like micelles was calculated using the tool "segmented line" (green), evaluating 100 worm-like micelles.

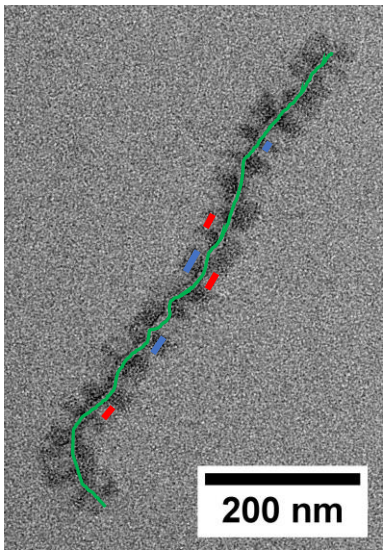

Fig. S7. Determination of patch size (PS: blue; PDxA: red) and length (green) of the worm-like micelles using the software *ImageJ*.

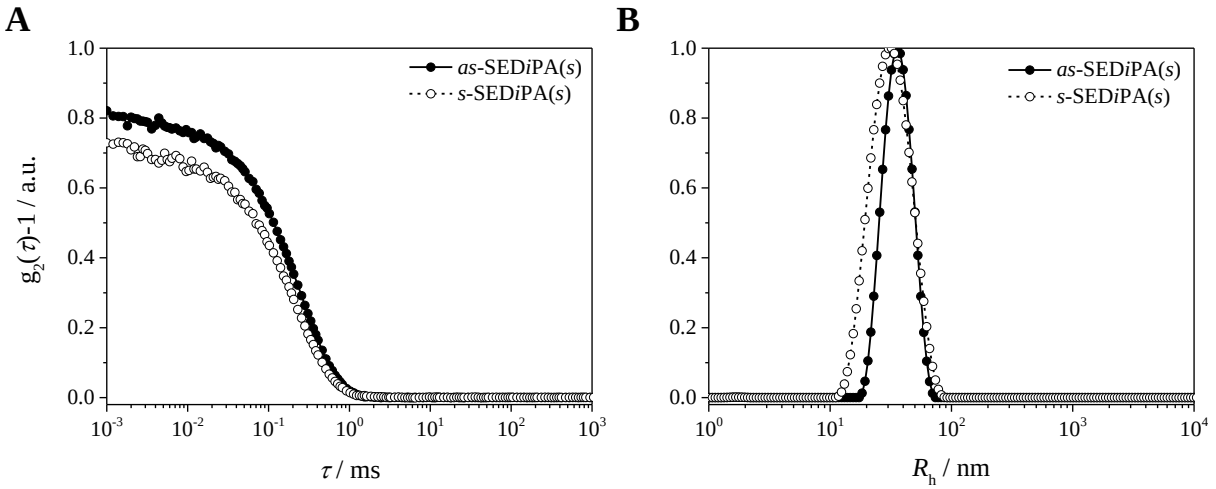

Fig. S8. DLS measurements of the *s*CCMs (c = 0.1 g·L^{-1}, dioxane) at a scattering angle of θ = 90°. A) Auto-correlation functions and B) unweighted hydrodynamic radii distributions (CONTIN analysis, R_h (*s*-SED*i*PA(*s*)) = 31.4 ± 0.3 nm and R_h(*as*-SED*i*PA(*s*)) = 35.8 ± 0.3 nm).

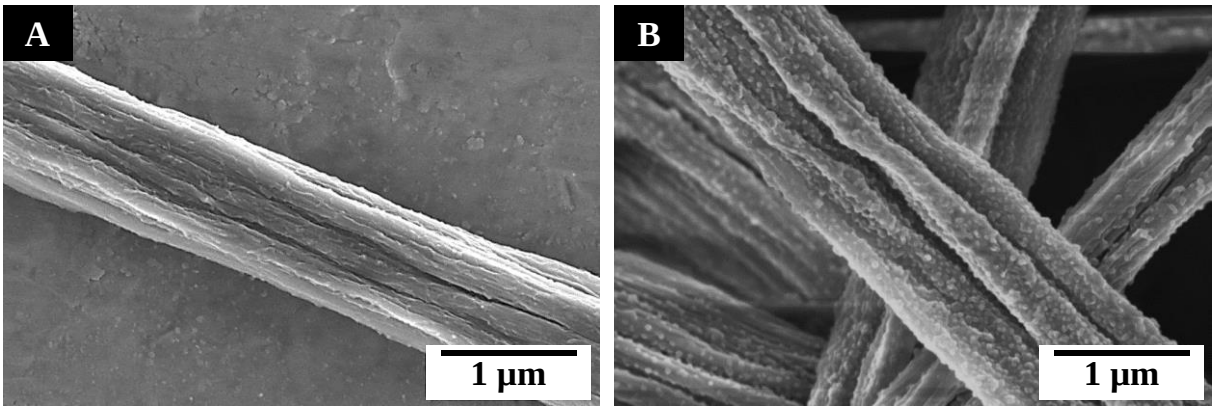

Fig. S9. SEM micrographs of patchy nonwovens. A) NW_*as*-SED*i*PA(*w*), B) NW_*as*-SED*i*PA(*s*).

Evaluation of the reaction kinetics according to the classical pseudo 1st order kinetics model. Due to the large excess of *n*-butanol (*n*-BuOH) compared to silane, a pseudo 1st order kinetics can be assumed. Consequently, the apparent reaction rate constants (k_{app}) can be calculated from the slope in the linear range of the corresponding 1st order kinetics plot as follows (Fig. S10):

$$-\frac{d[E]}{dt} = k \cdot [E] \cdot [n\text{-BuOH}] \quad \text{with } [E] = [silane] \tag{S2}$$

introducing $$k_{app,\,classical} = k \cdot [n\text{-BuOH}] \tag{S3}$$

results in $$-\frac{d[E]}{dt} = k_{app,\ classical} \cdot [E] \tag{S4}$$

integration gives $$-\ln\left(\frac{[E]}{[E]_0}\right) = k_{app,\ classical} \cdot t \tag{S5}$$

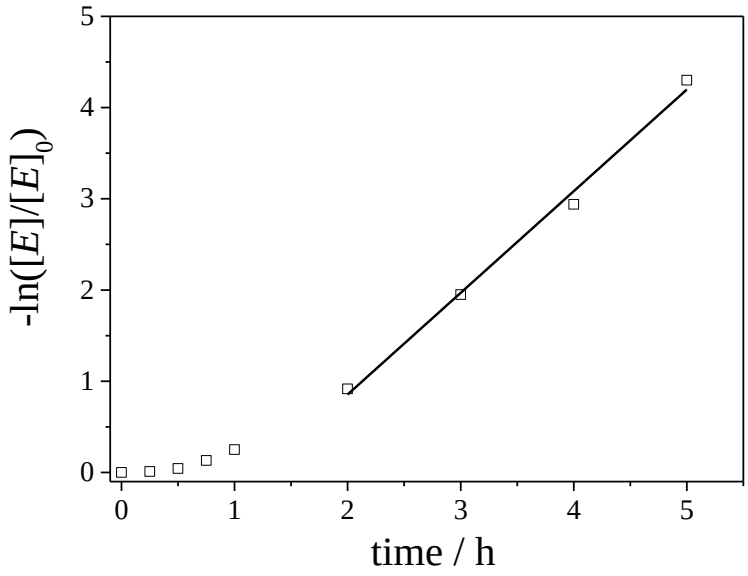

Fig. S10. Kinetics plot for the catalytic alcoholysis of dimethylphenylsilane with the Au NP-loaded patchy nonwoven NW_*s*-SED*i*PA(*w*)/Au, showing the determination of the apparent rate constants ($k_{app,\ classical}$) according to the classical 1st order kinetics model (squares: experimental data, line: linear fit according to eqn (S5)). An accurate fit is possible only for the second half of the observation period, where the plot shows a constant slope.

The reaction rate constants *k*, normalized to the concentration of *n*-butanol ([*n*-BuOH] = 10.93 mol·L^{-1}) and the overall surface area of the embedded Au NPs ($S_{NP,total}$), were determined from eqn (S6). The total NP surface area ($S_{NP,total}$, eqn (S7 – S10)) was calculated on the basis of the Au NP´s mean diameter (D_{TEM} = 9.5 ± 2.4 nm), the Au content in the hybrid nonwovens ($m_{Au,\ UV\text{-}Vis\ 400nm}$, Table 2) and the density of Au (ρ_{Au} = 19.32 g·cm^{-3}). The errors for $S_{NP,total}$ (eqn S11) and *k* (eqn S12) were calculated based on error propagation.

$$k = \frac{k_{app}}{[n\text{-BuOH}] \cdot S_{NP,total}} \tag{S6}$$

with $$S_{NP,total} = S_{NP,single} \cdot N_{NP} \tag{S7}$$

where $$S_{NP,single} = \pi \cdot {D_{TEM}}^2 \tag{S8}$$

and $$N_{NP} = \frac{m_{NP}}{\frac{4}{3} \cdot \pi \cdot \left(\frac{D_{TEM}}{2}\right)^3 \cdot \rho_{Au}} \tag{S9}$$

leads to $$S_{NP,total} = \frac{6 \cdot m_{NP}}{\rho_{Au}} \cdot \frac{1}{D_{TEM}} \tag{S10}$$

with $$\Delta S_{NP,total} = \sqrt{\left(-\frac{6 \cdot m_{NP}}{\rho_{Au}} \cdot \frac{1}{(D_{TEM})^2}\right)^2 \cdot (\Delta D_{TEM})^2} \quad \text{(S11)}$$

and $$\Delta k = \sqrt{\left(\frac{1}{[n\text{-BuOH}] \cdot S_{NP,total}}\right)^2 \cdot (\Delta k_{app})^2 + \left(-\frac{k_{app}}{[n\text{-BuOH}]} \cdot \frac{1}{(S_{NP,total})^2}\right)^2 \cdot (\Delta S_{NP,total})^2} \quad \text{(S12)}$$

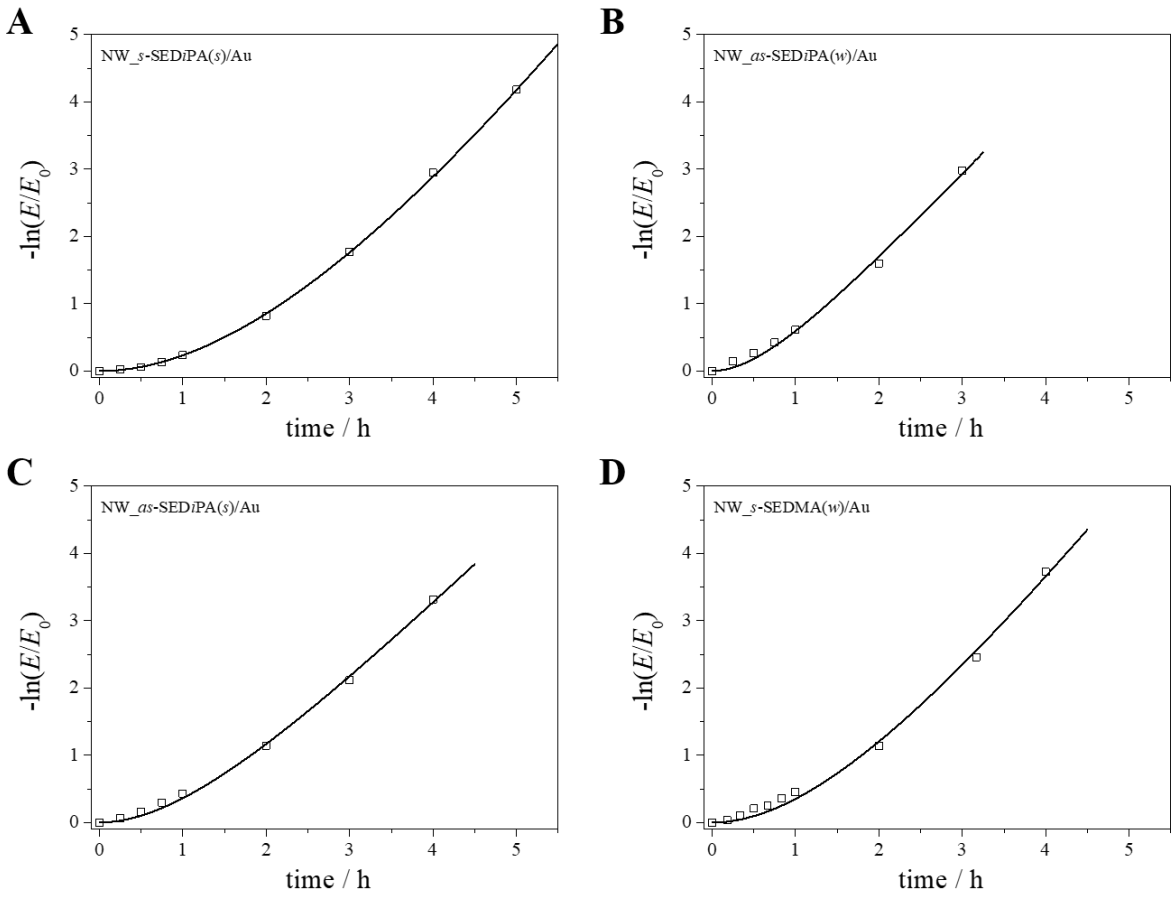

Fig. S11. Kinetics plot for the catalytic alcoholysis of dimethylphenylsilane with Au NP-loaded patchy nonwovens (squares: experimental data, line: fit according to our extended pseudo 1st order kinetics model (eqn (5)).

Table S2. Comparison of the apparent rate constants (k_{app}) and the corresponding normalized rate constants (k), determined using the classical and the extended 1st order kinetics model, respectively.

hybrid nonwovens	k_{app} [a] [h^{-1}]	k [b] [$L \cdot m^{-2} \cdot mol^{-1} \cdot s^{-1}$]	$k_{app,\ classical}$ [c] [h^{-1}]	$k_{classical}$ [b] [$L \cdot m^{-2} \cdot mol^{-1} \cdot s^{-1}$]
NW_*s*-SED*i*PA(*s*)/Au	1.77 ± 0.10	$(1.97 \pm 0.51) \cdot 10^{-2}$	1.21 ± 0.02	$(1.34 \pm 0.34) \cdot 10^{-2}$
NW_*s*-SED*i*PA(*w*)/Au	1.54 ± 0.11	$(2.10 \pm 0.55) \cdot 10^{-2}$	1.11 ± 0.06	$(1.52 \pm 0.39) \cdot 10^{-2}$
NW_*as*-SED*i*PA(*s*)/Au	1.18 ± 0.10	$(1.19 \pm 0.31) \cdot 10^{-2}$	1.09 ± 0.06	$(1.10 \pm 0.28) \cdot 10^{-2}$
NW_*as*-SED*i*PA(*w*)/Au	1.27 ± 0.11	$(1.20 \pm 0.32) \cdot 10^{-2}$	1.18 ± 0.11	$(1.12 \pm 0.30) \cdot 10^{-2}$
NW_*s*-SEDMA(*w*)/Au	1.55 ± 0.26	$(1.56 \pm 0.47) \cdot 10^{-2}$	1.28 ± 0.11	$(1.30 \pm 0.34) \cdot 10^{-2}$

[a] determined according to eqn (5) (extended 1st order kinetics model). [b] rate constant normalized to the surface of the embedded Au NPs (S_{AuNP}, Table 2) and the concentration of *n*-BuOH ($c_{n\text{-}BuOH}$ = 10.93 $mol \cdot L^{-1}$). [c] calculated using the classical 1st order kinetics model (eqn (S5), Fig. S10).

Table S3. Comparison of the obtained kinetic parameters for the alcoholysis of dimethyl-phenylsilane with *n*-BuOH with literature data.

catalyst	Au [d] [mol-%]	D [e] [nm]	time [h]	temp. [°C]	x_p [f] [%]	recyclability	Reference
NW_SEDxA(*w*)/Au	0.18	9.5	4-5	25	>99	>99% 10 cycles	this work
Au NP-loaded patchy nonwoven	0.1	11	7	25	>99	>99% 10 cycles	2
Au-containing PPX nanotubes	6.6	9.5	26	25	>99	>99% 18 cycles	3
Au/Al_2O_3	20	3-5	3	100	99	n/a	4
10Dod-Au NP array [a]	0.02	9	1	25	83	95% 3 cycles	5
Au/HAP_{nano} [b]	0.05	3	0.33	25	>99	>99% 3 cycles	6
PSSH@Au NP [c]	0.06	15-24	5	25	>99	n/a	7

[a] dodecanethiol self-assembled-monolayer-capped Au NPs. [b] nanohydroxyapatite-supported Au NPs. [c] with toluene as co-solvent. [d] relative to silane. [e] average diameter of Au NPs. [f] conversion.

References

1 T. Hendel, M. Wuithschick, F. Kettemann, A. Birnbaum, K. Rademann, J. Polte, *Anal. Chem.*, 2014, **86**, 11115–11124.

2 Schöbel, J.; Burgard, M.; Hils, C.; Dersch, R.; Dulle, M.; Volk, K.; Karg, M.; Greiner, A.; Schmalz, H. *Angew. Chem. Int. Ed.* **2017**, *56*, 405–408.

3 Mitschang, F.; Schmalz, H.; Agarwal, S.; Greiner, A. *Angew. Chem. Int. Ed.* **2014**, *53*, 4972–4975.

4 Raffa, P.; Evangelisti, C.; Vitulli, G.; Salvadori, P. *Tetrahedron Lett.* **2008**, *49*, 3221–3224.

5 Taguchi, T.; Isozaki, K.; Miki, K. *Adv. Mater.* **2012**, *24*, 6462–6467

6 Mitsudome, T.; Yamamoto, Y.; Noujima, A.; Mizugaki, T.; Jitsukawa, K.; Kaneda, K. *Chem. Eur. J.* **2013**, *19*, 14398–14402.

7 Kronawitt, J.; Fan, Z.; Schöttle, M.; Agarwal, S.; Greiner, A. *ChemNanoMat* **2019**, 5, 181-186.